



# Efficient magneto-optical TE/TM mode converter in a hybrid structure made with a SiO<sub>2</sub>/ZrO<sub>2</sub> layer coated on an ion-exchanged glass waveguide

Mounir Bouras\*, Mouad Mezhoud, Abdesselam Hocini

Laboratoire d'Analyse des Signaux et Systèmes, Department of Electronics, Université Mohamed Boudiaf-M'sila, BP.166, Route Ichebilila, M'sila, 28000, Algeria

## ARTICLE INFO

### Article history:

Received 8 February 2017

Accepted 22 November 2017

### Keywords:

Magneto optic  
Ion-exchanged glass  
Hybrid waveguide  
Isolator optics

## ABSTRACT

The TE-TM mode conversion is an important requirement for magneto-optical waveguide devices. In this work, we report on the theoretical study of magneto-optical waveguides on an ion-exchanged glass waveguide. This study explores the possibility to realize a mode converter TE-TM on a hybrid structure. This hybrid device is made by coating a SiO<sub>2</sub>/ZrO<sub>2</sub> layer doped with magnetic nanoparticles on an ion-exchanged glass waveguide. It has been analyzed by means of a beam propagation method for numerical solution of the full-vectorial wave equation. We have also used the transparent boundary condition. The mode converters TE-TM based on the Faraday rotation and modal birefringence are then numerically simulated. Depending on the increasing of nanoparticles volume fraction in the SiO<sub>2</sub>/ZrO<sub>2</sub> layer and on decreasing the modal birefringence of the hybrid structure, the TE-TM conversion efficiency varies from several percent to several tens of percent.

© 2017 Published by Elsevier GmbH.

## 1. Introduction

In the framework of optical telecommunication systems, the conception of integrated optic devices which allow a high speed data transmission requires the integration of elements that have a nonreciprocal effect such as optical isolators and circulators [1]. Optical isolators are very important components to prevent destabilization of laser source with reflected light. Faraday rotation is the standard physical principle to obtain non-reciprocity in such components [2]. Currently, the material widely used in bulk optical isolators is the ferrimagnetic garnet oxide crystal Yttrium Iron Garnet (YIG), or bismuth substituted yttrium iron garnet (Bi:YIG), deposited on a gadolinium gallium garnet (GGG) as substrate [5]. This substrate is not commonly used to realize integrated functions. Furthermore, the realization of YIG thin films which can requires an annealing temperature as high as 700 °C to be magneto active [3]. This temperature required for the crystallization of magnetic iron garnet is usually too high, it is evidently not so compatible with integrated optical technologies [4]. To overcome this problem, many studies are currently carried-out to develop magneto-optical materials compatible with existing integrated optics technologies. The first deals with the bonding of high quality Ce–YIG layers on classical substrate: glass or silicon [6,7]. The second is the development of novel magneto-optical materials compatible with classical technologies. Thus Zayets and

\* Corresponding author.

E-mail address: [mouno.25000@yahoo.fr](mailto:mouno.25000@yahoo.fr) (M. Bouras).

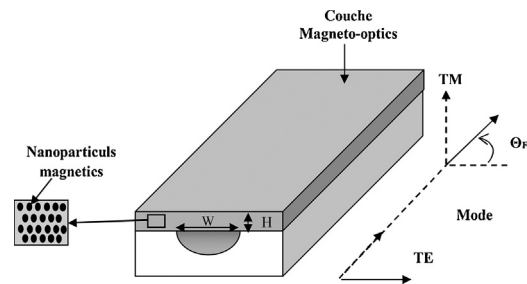


Fig. 1. Schematic of the integrated magneto-optical mode converter.

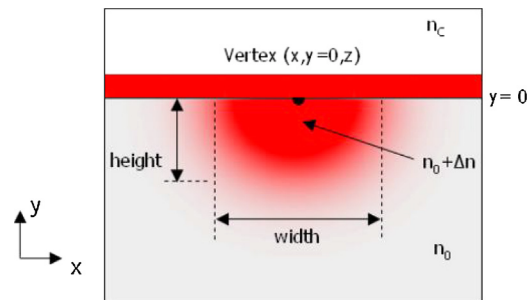


Fig. 2. Cross-section of the built-in 3D diffused hybrid structure.

all. have recently demonstrated a complete magneto-optical mode conversion in Cd<sub>1-x</sub>Mn<sub>x</sub>Te waveguide on GaAs substrate. In this way, lots of efforts have been made to obtain such materials compatible with semiconductor substrate [7–11], but few concern glass substrate. The group [10], has developed novel approach based on a composite magneto-optical matrix compatible with glass substrate. The films realized through a soft chemistry sol gel process, thin films can be obtained by dip coating on several substrates (silicon, glass) and silica type matrix is doped by magnetic nanoparticles. Such magneto-optical matrix has shown promising potentialities illustrated by a specific Faraday rotation of 199°/cm (@1550 nm) with a nanoparticles volume fraction of 1% [1]. A full compatibility with these substrates is provided by the soft thermal treatment required [1].

In this work we are using hybrid structure based composite magneto-optical layer on an ion-exchanged glass waveguide as shown on Fig.1. And can be used with glassy integrated circuits in order to realize hybrid mode converter.

We have this technology can produce high quality integrated optical components and which is one of the prominent technologies in the field of integrated optics, such as isolators and circulators. In previous works [12], the coupling coefficient being 26°/cm, with the birefringence value of  $7,7 \times 10^{-4}$ , it gives a modal conversion of 1.7° for a propagation length of 1 mm.

Z-independent magneto-optic waveguides have been analyzed and simulated by several methods such as: finite differences (FD) [13], the Galerkin method [14], and periodic Fourier transform [15]. The beam propagation method (BPM) is one of the favorite approaches used in the modeling and simulation of electromagnetic wave propagation in guided wave optoelectronic and fiber optic devices [16].

In this paper we report how to obtain a hybrid mode propagation presenting a best lateral confinement and realize efficient magneto-optical mode converter in a hybrid structure based on ion exchange glass technology. We have used the finite difference beam propagation method (FD-BPM) for simulation of the performance of a hybrid magneto-optical mode converter. This has been done through simulations using RSOFT CAD<sup>TM</sup>, a photonic design software, by RSoft Design Group, Inc.

## 2. Hybrid structure

Schematic structure of the hybrid structure ion-exchange device is presented in Fig.1 The hybrid waveguides structure composed into two parts: the first part is active layer, which are produced through the deposition of a magneto optic waveguide film onto the substrate. The second part is gradient waveguides, which are produced through the modification of optical substrate. Gradient waveguides are produced in the processes of ion-exchange in glass [17].

Ion-exchanged glass waveguides technology has largely demonstrated its capacity to realize integrated optical functions with compactness, stability, and low losses [2,17].

In order to achieve better depth confinement of the mode, an ion-exchanged layer was introduced to form a planar waveguide in the top surface of the second sample. Fig. 2.

In Table 1 the active couched of waveguide produced the flexibility of the refractive index will be helpful to suit the optical characteristics of the magneto-optical film with requirements of the desired application [2,17]. This is produced with

**Table 1**

(a) Refractive index of the host matrix at  $\lambda = 1550$  nm [2]. (b) Maximum power conversion  $R_M$  and propagation length of the hybrid structure waveguide a specific Faraday rotation of  $\theta_F = 155^\circ/\text{cm}$  at  $\lambda = 1550$  nm. (c) The maximum power conversion  $R_M$  and propagation length  $L_c$  in  $\text{SiO}_2/\text{ZrO}_2$  layer doped with magnetic nanoparticles  $\text{CoFe}_2\text{O}_4$  of the hybrid structure waveguide for modal birefringence  $\Delta N = 3,8 \times 10^{-4}$  at  $\lambda = 1550$  nm.

(a)		
Ratio $\text{SiO}_2/\text{ZrO}_2$ or $\text{TiO}_2$	Precursors	index@1550 nm
Sol 10/3	$\text{SiO}_2/\text{ZrO}_2$	1.504
Sol 10/7	$\text{SiO}_2/\text{ZrO}_2$	1.515
Sol 10/10	$\text{SiO}_2/\text{ZrO}_2$	1.528
Sol 10/12	$\text{SiO}_2/\text{TiO}_2$	1.580
Sol 10/10	$\text{SiO}_2/\text{TiO}_2$	1.575

(b)				
	$\Delta N$	$K$ ( $^\circ/\text{cm}$ )	$R_M$ ( $^\circ$ )	$L_c$ (mm)
Calculated by Formula (13) and (14)	$3,8 \times 10^{-4}$	90	2.85	0.764
BPM Method [Our work]	$3,8 \times 10^{-4}$	90	2.88	0.760
Hadi [2]	$7,7 \times 10^{-4}$	26	1.6	1
Garayt [12]	$2,6 \times 10^{-4}$	26	5.5	1.1

(c)				
Concentration	$\theta_F$ ( $^\circ/\text{cm}$ )	$K$ ( $^\circ/\text{cm}$ )	$R_M$ ( $^\circ$ )	$L_c$ (mm)
$\Phi = 0.70$ %	199	90	2.85	0.764
$\Phi = 1.00$ %	309	108	4.10	0.758
$\Phi = 1.50$ %	375	124	5.30	0.754
$\Phi = 2.04$ %	420	139	7.10	0.748

sol–gel technology, and by adjusting the molar ratio of metallic precursors the refractive index of the material can be of 1.50–1.575 [2].

The diffused profile is defined as [14]

$$n(x, y) = n_0 + [\Delta n g(x) f(y)]^\gamma \tag{1}$$

Where:

$$g(x) = 0.5 \left\{ \text{erf} \left[ \frac{(w/2 + x)}{h_x} \right] + \text{erf} \left[ \frac{(w/2 - x)}{h_x} \right] \right\} \tag{2}$$

Here,  $n_0$  is the substrate or background index,  $\Delta n$  is the maximum index change produced by diffusion from an infinitely extended source,  $w$  is the width of the source in the horizontal direction, and  $h_x$  and  $h_y$  are the diffusion lengths in the horizontal and vertical direction respectively ( $h_x = h_y$ ).

The vertical profile  $f(y)$  is determined by: [14]

$$f(y) = \exp \left[ -y^2/h_y^2 \right] \tag{3}$$

The parameter  $\gamma$  which equals 1.0 by default [18]. Since it represents the non-linear interaction between the concentration and index, it is applied after the index changes for all components that have been accumulated.

### 3. Magneto-optical hybrid waveguide theory

In the guiding film of the planar waveguide for the nonreciprocal hybrid structure, the magnetization is adjusted in the film plane perpendicular to the propagation direction, so that the dielectric tensor is [10,19].

$$\epsilon = \begin{pmatrix} \epsilon_{xx} & i\epsilon_{mo} & 0 \\ -i\epsilon_{mo} & \epsilon_{yy} & 0 \\ 0 & 0 & \epsilon_{zz} \end{pmatrix}_{\text{oxyz}} \tag{4}$$

Where  $\epsilon_{xx}$ ,  $\epsilon_{yy}$ ,  $\epsilon_{zz}$  and  $\epsilon_{mo}$  are the dielectric constants in the x, y, z directions and off-diagonal element, respectively. The sign of  $\epsilon_{mo}$  changes if the magnetization is reversed. For the TM modes, propagating along the z-direction, with longitudinal phase constant  $\beta$ , the electric and magnetic fields are:

$$\vec{E} = (E_x, 0, E_z) \exp [j (\omega t - \beta z)] \tag{5}$$

$$\vec{H} = (0, H_y, 0) \exp [j (\omega t - \beta z)] \tag{6}$$

$H_y$  can be derived from the Helmholtz differential equation [20]

$$\left\{ (\partial^2 / \partial x^2) + (k_0^2 \epsilon_{\text{eff}} - (\epsilon_y / \epsilon_x) \beta^2) \right\} H_y = 0 \tag{7}$$

Where the effective dielectric constant is given  $\epsilon_{\text{eff}} = \epsilon_z - (\xi^2 / \epsilon_x)$  For simplicity, it is assumed that  $\epsilon_x = \epsilon_z$  For the TM modes, the characteristic equation is [20,21]:

$$h \sqrt{k_0^2} = \tan^{-1} \left[ \left( \epsilon_{\text{eff}} / \sqrt{k_0^2} \right) \left( \left( \sqrt{\beta^2} \right) / \epsilon_c - \left( (\beta \xi) / (\epsilon_{\text{eff}} \epsilon_x) \right) \right) \right] + \tan^{-1} \left[ \left( \epsilon_{\text{eff}} / \sqrt{k_0^2} \right) \left( \left( \sqrt{\beta^2} \right) / \epsilon_s - \left( (\beta \xi) / (\epsilon_{\text{eff}} \epsilon_x) \right) \right) \right] \tag{8}$$

Where  $h$  is the film thickness.

Due to the presence of the off-diagonal element  $\epsilon_{\text{mo}}$  a coupling from TE to TM mode takes place in the structure and then a TE/TM mode conversion is created during the propagation. For propagation along Oz direction, the expression of the TE/TM coupling coefficient  $K$  is given by [18].

$$K = (i \cdot \omega \cdot \epsilon_0) / (4 \sqrt{P_{\text{TE}}}) \iint E_y^{\text{TE}*} \cdot \epsilon_{\text{MO}} \cdot E_x^{\text{TM}} dx \cdot dy = i \theta_F \eta_{\text{MO}} \tag{9}$$

$P_{\text{TE}}$ ,  $P_{\text{TM}}$  are the power associated to TE and TM modes respectively.  $\omega$  is the frequency corresponding to the vacuum wavelength  $\lambda$ .  $\epsilon_{\text{MO}}$  is linked to the refractive index  $n$  of the magneto-optical layer and to its specific Faraday  $\theta_F$  rotation through.  $\eta_{\text{MO}}$  is the magneto-optics confinement factor [12].

$$\epsilon_{\text{MO}} = (n \cdot \lambda \cdot \theta_F) / \pi \tag{10}$$

From the coupling coefficient  $K$  and using mode coupling theory, one can express the TE/TM mode conversion efficiency as a function of the propagation distance  $z$  [12,22–24].

$$R(z) = \left[ k_F^2 / \left( k_F^2 + (\Delta\beta/2)^2 \right) \right] \sin^2 \left[ \sqrt{k_F^2} z \right] \tag{11}$$

$\Delta\beta$  ( $^\circ/\text{cm}$ ) is the phase mismatch between TE and TM mode

$$\Delta\beta = 2\pi \Delta N / \lambda_{\text{TE}} \tag{12}$$

Where  $\Delta N$ , the modal birefringence. Due to the non-zero value of  $\Delta N$ , the conversion efficiency is limited to the maximum value  $R_M$  [12,17,22–24].

$$R_M = k_F^2 / \left( k_F^2 + (\Delta\beta/2)^2 \right) \tag{13}$$

Which is reached at a distance of

$$L_c = \pi / (4k_F^2 + \Delta\beta^2) \tag{14}$$

This equation highlights the main role played by the phase mismatch on the efficiency of the mode conversion. Contrary to the free space configuration and even if the material constituting the waveguide is anisotropic; the mode conversion is not 100% efficient. The guided configuration produces a geometric modal birefringence which decreases the mode conversion. It is thus necessary to control and decrease as much as possible this modal birefringence [12,17,22].

#### 4. Numerical results

The device design has been carried out with full-vectorial beam propagation method, using a mode solver (beamprop from RSOFT CADTM), of the boundary conditions used for the simulations. The device is shown schematically in Fig.1. The refractive index of the ion-exchanged waveguide varies from 1.58 at the surface to 1.50 in the deep substrate (@1550 nm) [12,17]. These values are close to that of the magneto-optical layer  $n = 1.51$  [12,17]. That should insure a good hybrid distribution of light in the structure.

##### 4.1. Achieve a TE/TM mode conversion in a hybrid structure

Fig. 2 shows the profiles of the TE0 and TM0 mode of a typical hybrid structure waveguide. The parameters are listed in the figure caption. Note the discontinuity of the electric field at the vertical boundaries.

The field distribution in the hybrid structure waveguide for the TE and TM polarizations is shown in Fig. 3 for width 5  $\mu\text{m}$  and values of refractive index of the active layer  $n_f = 1.51$ .

The Fig. 3 presented shows a good interaction between the active layer and the ion-exchange waveguide, if the layer index is equal or slightly higher than ion-exchange waveguide index. The TE field slightly expands in the thinner film region, and this effect is more important as the width is reduced. The TM mode appears to be better confined in the central part of the hybrid waveguide [17].

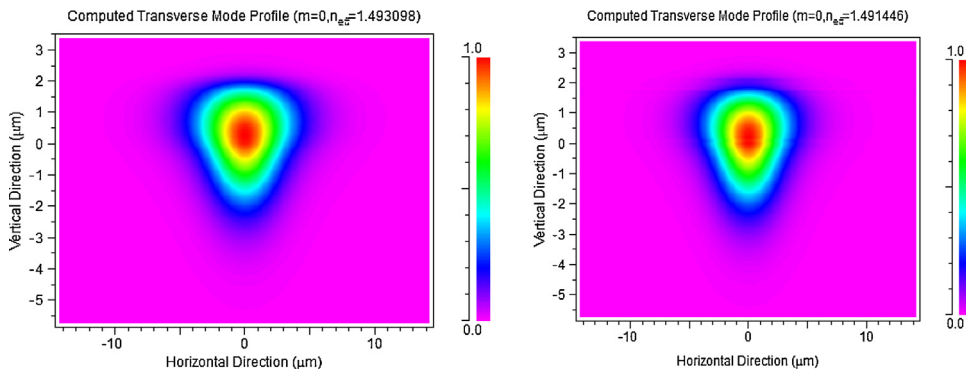


**Fig. 3.** Confinement of intensity in hybrid waveguide for TE and TM polarizations  $\eta_{MO} = 57\%$ , for guide width  $W = 5$  and  $H = 2 \mu\text{m}$  at  $\lambda = 1:55 \mu\text{m}$ .

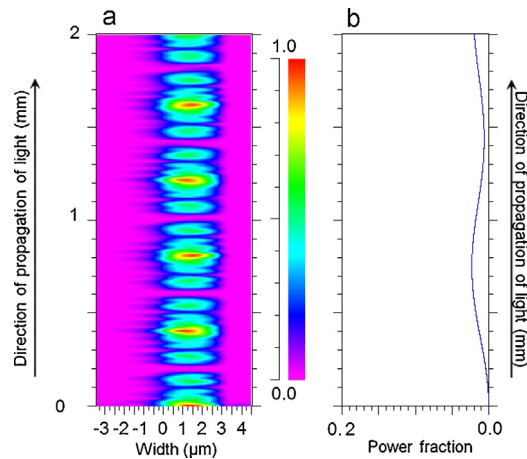


**Fig. 4.** Conversion efficiency RM in SiO<sub>2</sub>/ZrO<sub>2</sub> layer doped with magnetic nanoparticles CoFe<sub>2</sub>O<sub>4</sub> of the hybrid structure with concentration (0.7%) for modal birefringence  $\Delta N = 3,8 \times 10^{-4}$ . (a) Transverse electric field through the entire length. (b) Variation of power with length.

Fig. 4 gives the simulated mode conversion and the subsequent energy transfer mechanism between the transverse components TE and TM. The effects mode conversion caused by a periodic power transfer between TE and TM. At  $z = 0$ , the transverse component is only along the x direction, i.e.,  $TE = 0$ .

The magneto-optical mode conversion of the hybrid structure is reported in Fig. 4. The curve presents a nonreciprocal variation of the conversion mode as a function of the propagation direction, which is the typical behavior of the Faraday effect for a ferromagnetic material.

Thus, the result reported in Fig. 4 proves that it is possible to achieve a nonreciprocal mode conversion in a hybrid structure based on ion exchange glass technology. It confirms that the composite approach is a promising way to realize integrated nonreciprocal devices.

On Fig. 4, the coupling coefficient of the device was  $90^\circ/\text{cm}$ . combined with the birefringence value of  $3,8 \times 10^{-4}$ , it has given a modal conversion of  $2.88^\circ$  for a propagation length of  $0.764 \text{ mm}$ .

Table 1 presents a maximum power conversion  $R_M$  and propagation length  $L$  in SiO<sub>2</sub>/ZrO<sub>2</sub> layer doped with magnetic nanoparticles CoFe<sub>2</sub>O<sub>4</sub> for modal birefringence  $\Delta N = 3,8 \times 10^{-4}$  at  $\lambda = 1550 \text{ nm}$ .

The simulation results are consistent with the analytical calculations, the coupling coefficient and the modal birefringence has a great influence on the performance, and responsible for maximum power conversion  $R_M$ .

#### 4.2. Effect of the concentration of the nanoparticles in the guiding layer for a hybrid structure

In this section, we study the influence of the volume fractions of nanoparticles on mode conversion, the imaginary part of the off-diagonal parameters leads to this volume fraction and it has a great influence on the performance, and responsible for the Faraday rotation.

Figs. 5 and 6 present the variation of the TM–TE mode conversion RM as a function of different concentrations of hybrid structure, for four values of nanoparticles volume fraction, (0.7%, 1%, 1.5% and 2.04). The concentration of the fluid is an important factor which slightly affects the yield.

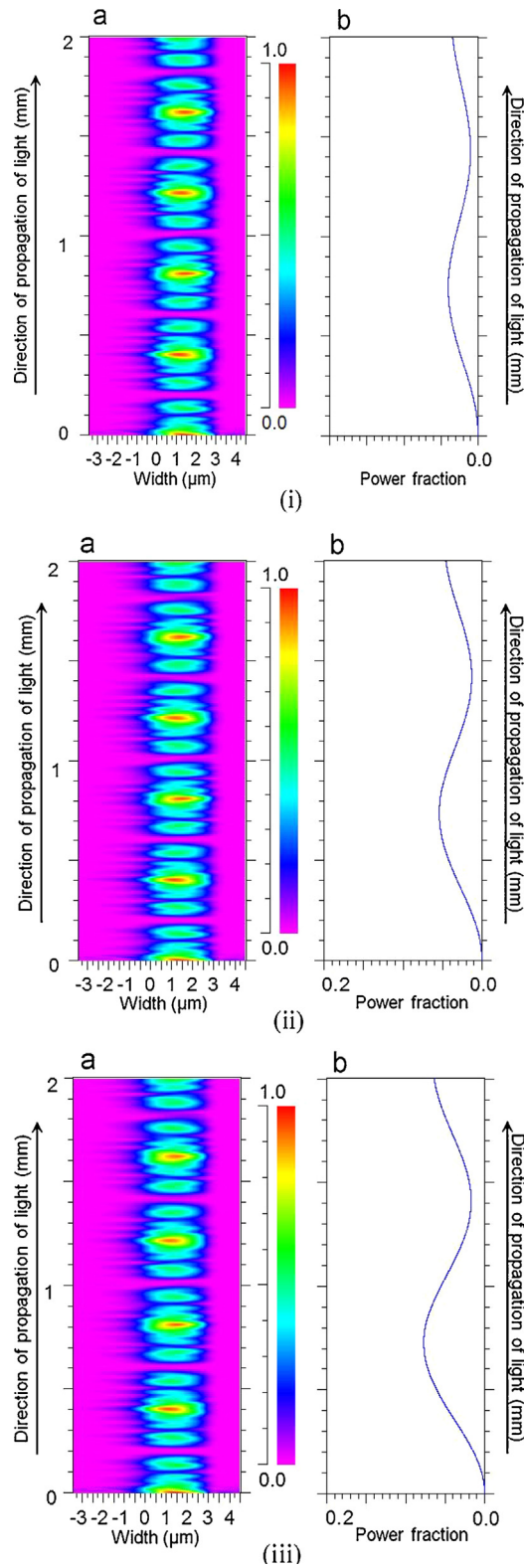


**Fig. 5.** Conversion efficiency  $R_M$  in  $\text{SiO}_2/\text{ZrO}_2$  layer doped with magnetic nanoparticles  $\text{CoFe}_2\text{O}_4$  of the hybrid structure with different concentrations (i) (1%), (ii) (1.5%) and (iii) (2.04%) for modal birefringence  $\Delta N = 3,8 \times 10^{-4}$ . (a) Transverse electric field through the entire length. (b) Variation of power with length.

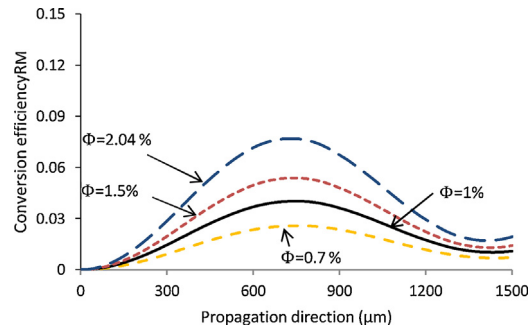


**Fig. 6.** Conversion efficiency  $R_M$  in  $\text{SiO}_2/\text{ZrO}_2$  layer doped with magnetic nanoparticles  $\text{CoFe}_2\text{O}_4$  of the hybrid structure with different concentrations (0.7, 1, 1.5 and 2.04%) for modal birefringence  $\Delta N = 3,8 \times 10^{-4}$ . The incident beam has a TE polarization.

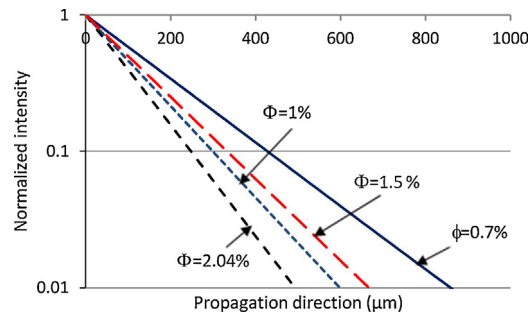


**Fig. 7.** normalized intensity of light as a function of propagation length.

This variation is proportional to the increase of concentrations, the conversion output increase. When the concentration is (0.7%), RM is equal to 2.85% but for a high value of the concentration (2.04%), RM is equal to 7.1%. These variations result from the increasing of off-diagonal parameter tensor, from increasing of concentrations.

Table 1 presents a maximum power conversion RM and propagation length L for modal birefringence  $\Delta N = 3,8 \times 10^{-4}$ .

The fluid concentration creates a change in the modal birefringence which increased conversion efficiency RM and reduces of propagation length L.

Fig. 7 presents normalized intensity of light as a function of propagation length of four values of volume fraction nanoparticles. The simulations presents the absorption of light in thin films hybrid structure of magnetic fluids using different concentrations and different thicknesses, whereas that the absorption increases with concentration and thickness. It is clear that as  $\phi$  increases, the optical absorption increases and the energy tends to zero.

One can easily check that this difference of magnitude respects the ratio of the nanoparticles concentration. But it seems interesting to note that the use a composite material with a small amount of magnetic particles in order to minimize the losses [12].

#### 4.3. Effect of the modal birefringence for the hybrid structure

Another factor influencing the mode conversion is the modal birefringence  $\Delta\beta$ , which is a major drawback to perform this conversion. The modal birefringence, is the difference between the TE and TM effective index for mode number m and  $\lambda$  is the light wavelength.

To improve the magnitude of the modal conversion and reach the  $45^\circ$  that are required for the realization of an optical isolator, the modal birefringence of the hybrid structure could be decreased. Consequently, in order to obtain good conversion efficiency, the modal birefringence must be as lower as possible.

In this work, an attempt was made to optimize the hybrid structure in order to obtain a lower birefringence value and lower loss. To confirm the two conditions, we use the geometrical parameter which fulfill the conditions, and single mode calculated from our previous work [17]. We study the mode conversion in hybrid waveguide structure component and we simulate the influence of geometrical parameters on the propagation length in the hybrid waveguide device.

Table 2 presents a maximum power conversion RM and propagation length L for different concentrations, which presented in the Fig. 8.

The Fig. 8 presents the specifics Faraday rotation being  $420^\circ/\text{cm}$  at concentration  $\Phi = 2.04\%$ . Combined with the lower birefringence value  $\Delta N = 125 \times 10^{-4}$ , it gives a modal conversion of 16% for a propagation length of 0.65 mm. This value is in good agreement with the one that has been previous simulation and reported in Fig. 6.

**Table 2**

The maximum power conversion  $R_M$  and propagation length  $L$  in  $\text{SiO}_2/\text{ZrO}_2$  layer doped with magnetic nanoparticles  $\text{CoFe}_2\text{O}_4$  of the hybrid structure waveguide for modal birefringence  $\Delta N = 125 \times 10^{-4}$  at  $\lambda = 1550$  nm.

Concentration	$\Delta N$	$\eta_{\text{Mo}}(\%)$	$K$ ( $^\circ/\text{cm}$ )	$R_M$ (%)	$L_c$ (mm)
$\Phi = 0.70$ %	$1,25 \times 10^{-4}$	19	29	3.6	760
$\Phi = 1.00$ %	$1,25 \times 10^{-4}$	17	34	4.5	754
$\Phi = 1.50$ %	$1,25 \times 10^{-4}$	16	42	7.8	730
$\Phi = 2.04$ %	$1,25 \times 10^{-4}$	14	63	16	650

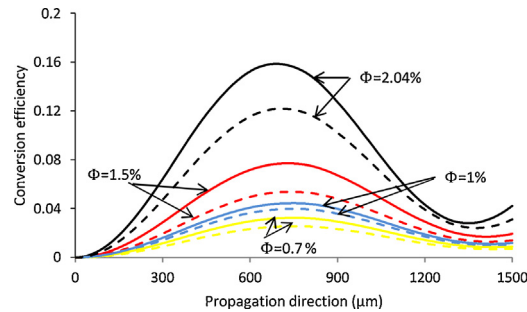


**Fig. 8.** Conversion efficiency  $R_M$  in  $\text{SiO}_2/\text{ZrO}_2$  layer doped with magnetic nanoparticles  $\text{CoFe}_2\text{O}_4$  of the hybrid structure with different concentrations (0.7, 1, 1.5 and 2.04%) for modal birefringence  $\Delta N = 125 \times 10^{-4}$ . The incident beam has a TE polarization.

## 5. Conclusion

In this article, we have designed and simulated a magneto-optical device based on a magnetic nanoparticles doped silica layer reported on ion-exchanged glass waveguide. The present work studied the possible to achieve a TE/TM mode conversion in an integrated hybrid structure made with composite silica-based magneto-optical layer coated on an ion exchange glass technology. We have used the BPM for numerical simulation of the propagation of optical pulses in the nonreciprocal hybrid structure. Propagation constant of the waveguide structure has been derived by using the effective index method. The maximum power conversion 16% obtained at a wavelength  $\lambda = 1550$  nm is limited by a quite low coupling coefficient and structure modal birefringence. These parameters are optimized via numerical simulations.

## References

- [1] F. Choueikani, F. Royer, D. Jamon, A. Siblini, J.J. Rousseau, N. Sophie, J. Charara, *Appl. Phys. Lett.* 94 (2009) 051113.
- [2] H. Amata, F. Royer, F. Choueikani, D. Jamon, F. Parsy, J.E. Broquin, S. Neveu, J.J. Rousseau, Hybrid magneto-optical mode converter made with a magnetic nanoparticles-doped  $\text{SiO}_2/\text{ZrO}_2$  layer coated on an ion-exchanged glass waveguide, *Appl. Phys. Lett.* 99 (2011) 251108.
- [3] M. Huang, Z.C. Xu, *Appl. Phys. A* 81 (2005) 193.
- [4] D.C. Hutchings, *J. Phys. D* 36 (2003) 2222.
- [5] N. Bahlmann, M. Lohmeyer, H. Dötsch, P. Hertel, *Electron. Lett.* 34 (1998) 2122.
- [6] Yuya Shoji, Tetsuya Mizumoto, Hideki Yokoi, Wei Hsieh, Richard M. Osgood Jr, Magneto-optical isolator with silicon waveguides fabricated by direct bonding, *Appl. Phys. Lett.* 92 (2008) 071117.
- [7] Anne-Laure Joudrier, Maurice Couchaud, Hubert Moriceau, Jean-Emmanuel Broquin, Bernard Ferrand, Jean-Luc Deschanvres, Direct bonding conditions of ferrite garnet layer on ion-exchanged glass waveguides, *Phys. Status Solidi (a)* 205 (10) (2008) 2313–2316.
- [8] H. Shimizu, M. Tanaka, Design of semiconductor-waveguide-type optical isolators using the nonreciprocal loss/gain in the magneto-optical waveguides having MnAs nan-ousters, *Appl. Phys. Lett.* 81 (2002) 5246–5248.
- [9] V. Zayets, M.C. Debnath, K. Ando, Optical isolation in CdMnTe magneto-optical waveguide grown on GaAs substrate, *J. Opt. Soc. Am. B* 22 (2004) 281–285.
- [10] A. Lesuffleur, M. Vanwolleghem, P. Gogol, B. Bartenlian, P. Beauvillain, J. Harmle, L. Lagae, J. Pistora, S. Visnovsky, R. Wirix-Speetjens, Magneto-optical parameters of  $\text{Co}_90\text{Fe}_{10}$  and  $\text{Co}_{50}\text{Fe}_{50}$  ferromagnetic thin films for  $1.3 \mu\text{m}$  integrated isolator, *J. Magn. Magn. Mater.* 305 (2006) 284–290.
- [11] M.R. Lebbal, et al., Anisotropy adjustment and thickness of thin layer doped by nanoparticles magnetic for the realization of phase matching between fundamental modes in monomode waveguides, *Eur. Phys. J. Appl. Phys.* 42 (2008) 75–80.
- [12] Jean Philippe Garayt, et al., Efficient magneto-optical mode converter on glass, *Proceedings Volume, Integrated Optics: Devices, Materials, and Technologies XVIII* (2014) 89880F, <http://dx.doi.org/10.1117/12.2037699>.
- [13] T.B. Koch, J.B. Davies, D. Wickramasinghe, Finite element/finite difference propagation algorithm for integrated optical device, *Electron. Lett.* 25 (1989) 514–516.
- [14] M. Shamonin, P. Hertel, Analysis of nonreciprocal phase shifters for integrated optics by a Galerkin method, *Opt. Eng.* 34 (1995) 849–852.
- [15] K. Watanabe, K. Kuto, Numerical analysis of optical waveguides based on periodic Fourier transform, *Prog. Electromagnet. Res. PIER* 64 (2006) 1–21.
- [16] M. Khatir, N. Granpayeh, Design and simulation of magneto-optic Mach-Zehnder isolator, *Optik* 122 (2011) 2199–2202.
- [17] A. Hocini, M. Bouras, H. Amata, Theoretical investigations on optical properties of magneto-optical thin film on ion-exchanged glass waveguide, *Opt. Mater.* 35 (2013) 1669–1674.
- [18] [www.rsoftdesign.com](http://www.rsoftdesign.com).
- [19] R. Chen, D. Tao, H. Zhou, Y. Hao, J. Yang, Asymmetric multimode interference isolator based on nonreciprocal phase shift, *Opt. Commun.* 282 (5) (2009) 862–866.
- [20] X. Gao, J.A. Woollam, R.D. Kirby, D.J. Sellmyer, C.T. Tanaka, J. Nowak, Dielectric tensor for magneto-optic NiMnSb, *J.S. Moodera, Phys. Rev. B* 59 (1999) 9965.

- [21] S. Wittekoek, T.J.A. Popma, J.M. Robertson, P.F. Bongers, Magneto-optic spectra and the dielectric tensor elements of bismuth-substituted iron garnets at photon energies between 2.2–5.2 eV, *Phys. Rev. B: Condens. Matter* 12 (1975) 2777–2788.
- [22] M. Bouras, A. Hocini, Mode conversion in magneto-optic rib waveguide made by silica matrix doped with magnetic nanoparticles, *Opt. Commun.* 363 (2016) 138–144.
- [23] A. Hocini, A. Bouchelaghem, D. Saigaa, M. Bouras, T. Boumaza, M. Bouchemat, Birefringence properties of magneto-optic rib waveguide as a function of refractive index, *J. Comput. Electron.* 12 (2013) 50–55.
- [24] M. Lohmeyer, N. Bahlmann, O. Zhuromskyy, H. Dötsch, P. Hertel, *Opt. Commun.* 158 (1998) 189.